Stabilization of soft soils using electrochemical mineral precipitation: application to overburden dumps

Vandana Brar[1*], *Deepanshu* Shirole[1], *Sovik* Das[1], *David* Gregoire[2] and *Surajit* Sarkar[3]

[1] Department of Civil and Environmental Engineering, Indian Institute of Technology Delhi, Hauz Khas, New Delhi-110016
[2] Geomechanics and Porous Media (G2MP), University of Pau & Pays Adour (UPPA), Anglet, France-64600
[3] Natural Resources Division, Tata Steel Limited, Jamshedpur, Jharkhand, India-831001

Abstract. Mine overburden dumps (MOBD) are generally unstable due to poor compaction, high permeability, and a lack of internal cohesion, posing a significant risk of slope failure and environmental hazard. Therefore, developing an effective stabilization technique for MOBD is vital to ensure long-term safety and sustainable mining operations. One promising approach is the use of electrodeposition, which reduces permeability and enhances mechanical stability by inducing mineral precipitation within the pore spaces. When an electrical potential (EP) is applied across the MOBD, it drives the electrolysis of chemical compounds and the migration of ions toward the electrodes, leading to the formation of stable, insoluble compounds such as carbonates or silicate minerals. In this context, laboratory experiments were performed using calcium chloride and sodium metasilicate as wetting fluid in the MOBD sample. The EPs of 1 V, 3 V, and 5 V were selected to determine the efficacy of mineral precipitation at different potentials. Post-treatment characterization using scanning electron microscopy (SEM) confirmed the formation of calcium silicate hydrate as the primary electrodeposit across all voltages. However, the uniformity and extent of electrodeposition vary with the magnitude of EP: low voltage results in uniform electrodeposits, whereas high voltage leads to non-uniform electrodeposits. Moreover, an increase in strength of up to 70% was immediately measured via a penetration test for the treated samples. In conclusion, this study demonstrates the potential of electrodeposition in stabilizing MOBD.

1 Introduction

The increasing rate of urbanization has significantly increased mineral requirements, consequently leading to large-scale disturbance and removal of topsoil during extraction processes [1]. As a result of extensive extraction activities, the mining sector produces enormous quantities of waste material, with annual overburden generation estimated at 5–7 billion tons [2]. Consequently, these overburden materials are commonly deposited as dumps with steep, unstable slopes that are highly susceptible to erosion and shallow failures, leading to soil degradation, habitat disturbance, and possible water contamination. Additionally, overburden materials from metal ore, including copper and zinc, are often acidic and can release toxic elements through leaching when disposed of in landfills, thereby creating significant environmental pollution risks [1]. To address these challenges, it is essential to develop sustainable management strategies that promote the reuse, recycling, and valorization of mining waste. Approaches such as stabilization, incorporation into construction materials, or recovery of valuable metals can reduce ecological impacts while converting waste into economically beneficial resources [2, 3]. The purposes of stabilization include minimizing water infiltration, reducing the leaching of contaminants, and preventing erosion [1].

Traditional stabilization techniques are typical employed to improve the mechanical properties of overburden dumps, which primarily involves blending with conventional binders, such as fly ash, Portland cement [4]. Stabilizing mine tailings with Portland cement is highly carbon-intensive, releasing roughly one ton of CO_2 per ton of Portland cement produced. This makes the cement industry responsible for nearly 7 % of global greenhouse gas emissions [5]. Such emissions contribute substantially to climate change, underscoring the urgent need for alternative methods to stabilize overburden material that are both mechanically effective and environmentally sustainable. Consequently, electrodeposition through the application of mild electric potential (EP) has emerged [6]. The application of an EP to the sand in the presence of a chemical solution induces electrokinetic phenomena, such as electrolysis and ion electromigration [7]. Due to electrokinetic phenomena, nucleation and formation of electrodeposits take place in the pore space of sand [8]. To the best of the author's knowledge, this approach has been successfully employed to improve soil properties; it has not yet been applied to overburden materials [6, 8].

* Corresponding author: Vandana.Brar@civil.iitd.ac.in

In the present study, this technique is extended to overburden materials to investigate the effect of mild EP on the MOBD structure in the presence of (CC + NS) (calcium chloride and sodium metasilicate) as wetting fluids. The main aims of the present study are to examine the mineralogical changes with the application of different EPs. This study explores explicitly the influence of mild EP on the following variables that dominate the performance of MOBD across micro to macro scales: (i) the size, morphology, and chemical composition of the electrodeposits; (ii) the pH of the treated MOBD; and (iii) penetration resistance. The microscopic and macroscopic analysis will help elucidate the underlying mechanisms driving the mechanical behaviour of MOBD under the influence of a mild EP.

2 Materials and methods

2.1 Materials

The overburden dump material was procured from the Joda West mine dump of Tata Steel Ltd., located in Keonjhar, Odisha. Before testing, the grain size and texture composition of the MOBD sample was characterized through sieve analysis and hydro meter experiments (Fig. 1). Through this analysis, the MOBD sample was found to be a silt loam type of soil, and was composed of 30% sand, 55% silt, and 15% clay [10].

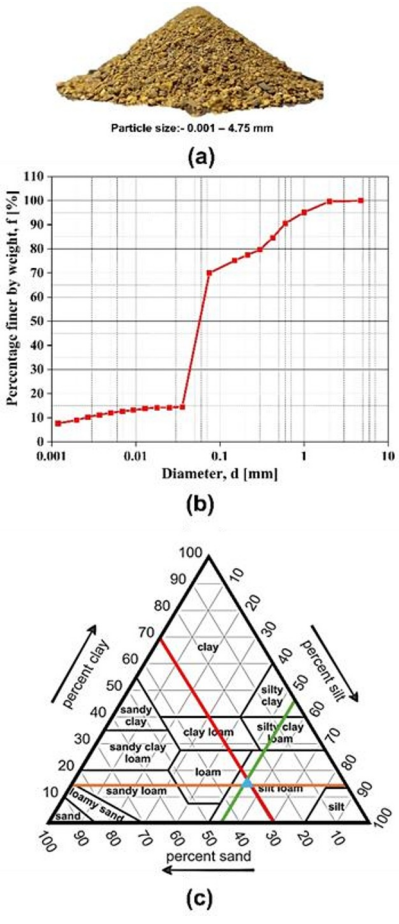

Fig. 1. (a) Overburden sample from Joda west mines; (b) grain size distribution curve; (c) USDA soil texture classification.

2.2 Methodology

For the electrical conditioning of the MOBD samples, an electrochemical reactor was indigenously prepared at IIT Delhi (Fig. 2). In the four electrochemical reactor, 50 g of MOBD samples with a relative density of 45 ± 5% were conditioned. Subsequent to the placement of the MOBD samples in the reactor, (0.5 cm × 0.5 cm × 0.2 cm) carbon-felt electrodes were strategically placed within the MOBD samples. Note that the samples were injected with 2 M calcium chloride (CC) and sodium metasilicate (SM) wetting fluid (WF) prior to the electrical conditioning. Specifically, four different magnitudes of EPs were applied across the carbon-felt electrodes using a DC power supply named as:
(i) 0 V MOBD sample with distilled water (MOBD0),
(ii) 1 V MOBD sample with WF (OBD1),
(iii) 3 V MOBD sample with WF (OBD2) and
(iv) 5 V MOBD sample with WF (OBD3)
For the reproducibility and reliability of the results, three samples were tested for each condition. The details of experimental conditions are presented in Table 1.

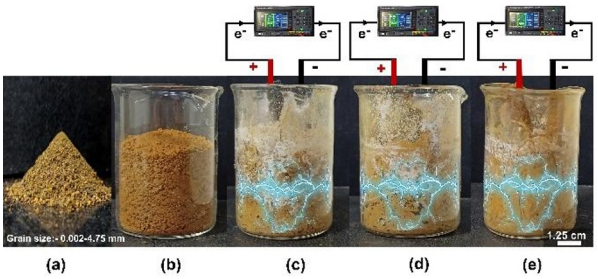

Fig. 2. Experimental setup of electrodeposition reactor (a) virgin OBD sample; (b) MOBD0 sample; (c) MOBD1 sample; (d) MOBD2 sample; and (e) MOBD3 sample.

Under the influence of voltage gradient, electrochemical reactions take place, leading to the formation of CSH (calcium-silicate-hydrate) gel, as shown in Equations 1-3 [10, 11]:

$$2H_2O \rightarrow O_2(\uparrow) + 4H^+ + 4e^- \quad (1)$$

$$2H_2O + 2e^- \rightarrow H_2(\uparrow) + 2OH^- \quad (2)$$

$$CaCl_2 + Na_2SiO_3 + H_2O \rightarrow CSH(\downarrow) + 2Na^+ + 2Cl^- \quad (3)$$

Table 1. Summary of the tests conducted for this study.

Tested material	Sample ID	Electrical conditioning: parameters		
		Wetting fluid (2 M)	Voltage gradient (V/cm)	Treatment duration (hours)
Mine overburden material (MOBD)	MOBD0	CC + SM	0	6
	MOBD1		1	
	MOBD2		3	
	MOBD3		5	

Following this, to evaluate the changes in the MOBD samples after electrical conditioning, optical analysis, penetration resistance tests, and ultrasonic measurements were conducted.

3 Result and discussion

3.1 Microstructural variation

The microstructure of the MOBD0, MOBD1, MOBD2, and MOBD3 samples was analysed using a compound and a scanning electron microscope (SEM) from JEOL JSM-7800F Prime, Japan, which provides a spatial resolution of up to 0.5 nm, as shown in Fig. 3. Prior to imaging, the samples were taken from the 1.2 cm depth of the sample, which were air-dried to remove residual moisture and mounted on the aluminium stubs using conductive carbon tape. To minimize charging effects and improve image quality, the specimens were coated with a thin conductive layer prior to analysis [13].

The untreated MOBD0 sample exhibited a loosely packed and heterogeneous microstructure, characterized by distinct clay and sand particles with visible intergranular voids. No evidence of mineral precipitates was observed on the particle surfaces, indicating the absence of bonding mechanisms in the untreated sample (Fig. 3(a)). However, after the injection of CC + NS under the application of 1 V EP in the MOBD1 sample, a marked transformation in microstructure was observed. Optical microscopy revealed the formation of a prominent, white-coloured compound coating the surfaces of both clay and sand particles (Fig. 3 (c)). Correspondingly, SEM images showed a dense, continuous, and relatively uniform gel-like amorphous matrix bridging adjacent particles (Fig. 3 (d)). From a previous study, this morphology resemble the characteristic of calcium silicate hydrate (CSH), which acts as a cementing agent by filling pore spaces and forming interparticle bonds, thereby contributing to improved mechanical integrity [14].

As the applied EP was increased to 3 V in the MOBD2 sample, a noticeable reduction in the quantity and continuity of electrodeposits was observed. While some cementitious material remained, the precipitates appeared more localized and less uniformly distributed across particle surfaces (Fig. 3(e)). The SEM images revealed disrupted and fragmented gel structures (Fig. 3 (f)). This can be attributed to the accelerated electrolysis and ion transport, leading to non-uniform precipitation and disruption of gel formation [8]. Upon further increasing the EP to 5 V in the MOBD3 sample, the surface morphology showed minimal white precipitates, with clay and sand particles becoming more exposed and exhibiting limited evidence of bonding material (Fig. 3(g, h)). The SEM image confirmed the presence of sparse, discontinuous deposits and a largely uncemented particle framework. This behaviour can be attributed to intensified electrolysis reactions and accelerated ion transport at higher voltages, which promote rapid ionic migration and localized supersaturation [15]. Such conditions can lead to non-uniform precipitation, premature nucleation, and subsequent disruption or dissolution of the gel-like CSH phase, thereby inhibiting effective particle bonding [7, 15].

Overall, the microstructural observations highlight the critical influence of applied electric potential on the nature, distribution, and stability of electrodeposited cementitious phases in MOBD. Moderate EP conditions favour uniform CSH formation and effective interparticle bonding, whereas excessive EP intensifies electrochemical reactions, thereby adversely affecting gel continuity and microstructural integrity.

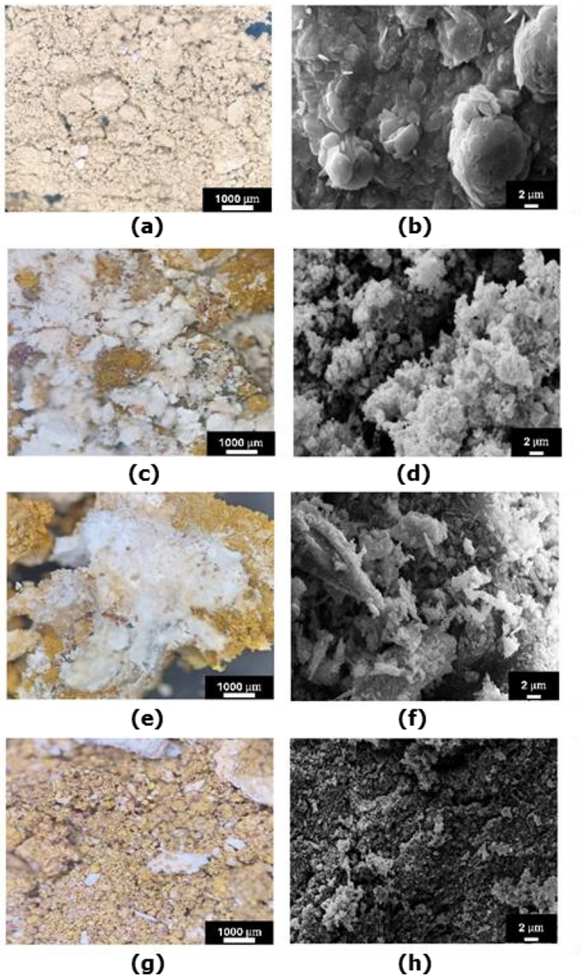

Fig. 3. Microscopic and SEM images of (a), (b) MOBD0 sample; (c), (d) MOBD1 sample; (e), (f) MOBD2 sample and (g), (h) MOBD3 sample.

3.2 Potential of hydrogen (pH) profile

The pH of the MOBD was measured both before and after electrodeposition using a portable Horiba Laquatwin pH meter with a measurement range of 0–14. For pH analysis, the samples were first sieved through a 2 mm mesh. A slurry was then prepared by mixing 20 ± 0.1 g of the sieved sample with an equal mass of deionized water, after which the suspension was allowed to equilibrate for one hour to achieve stable ionic redistribution before measurement.

Fig. 4 illustrates the effect of EP on the pH of different MOBD samples before and after electrodeposition. In the MOBD0 sample, the pH remained the same before and after treatment, indicating that precipitation-inducing ions are essential to cause any change in the pH of the WF. This observation is consistent with SEM results, which confirmed the lack of newly formed mineral phases in the MOBD0 sample.

In contrast, the MOBD1 sample exhibited a moderate reduction in pH, decreasing from 10.78 to 9.85 after electrodeposition. This decrease can be attributed to the combined effects of proton (H^+) generation during water electrolysis at the anode and the relatively neutral ionic behaviour of calcium chloride (CC) [17]. Furthermore, the observed pH reduction is likely influenced by the consumption of OH^- ions during the precipitation of calcium silicate hydrate. Such pH trends are in good agreement with an earlier study, which reported similar decreases in alkalinity associated with the CSH precipitation process [18].

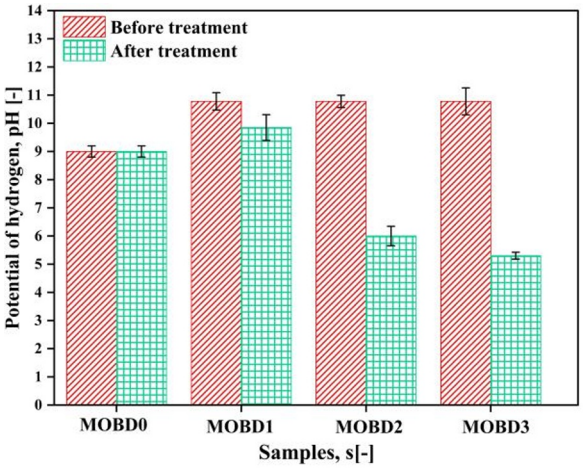

Fig. 4. Variation in the potential of hydrogen (pH) of MOBD before and after the electrodeposition at different EPs.

Conversely, a more pronounced pH reduction was observed in the MOBD2 sample, where the pH decreased substantially from 10.78 to 6. Similarly, in the MOBD3 sample, a decrease in pH from 10.78 to 5.3 was observed. This can be ascribed to the increased intensity of the electrolysis reaction [19]. This significant shift indicates an enhanced electrochemical reaction intensity, leading to greater ionic migration and increased generation of acidic species within the system. Similarly, the MOBD3 sample showed the largest decrease in pH, from 10.78 to 5.3, reflecting the strongest electrolysis effect among all samples. This behavior can be attributed to the higher applied EP, which intensified water electrolysis reactions and promoted greater accumulation of H^+ ions in the sample [16].

Overall, the progressive reduction in pH from MOBD0 to MOBD3 highlights the critical role of electrochemical conditions and reactive ion availability in governing the electrodeposition. These pH variations are expected to directly influence mineral precipitation mechanisms, microstructural development, and, ultimately, the mechanical performance of the treated samples.

3.3 Indirect stiffness measurements

For facilitating the preliminary insights into the mechanical behaviour of MOBD samples before and after the electrodeposition penetration resistance (P_r) was evaluated using the Vicat apparatus. Penetration-based measurements are particularly effective for assessing relative changes in surface hardness and bonding development in cemented or partially cemented materials. To evaluate the indirect stiffness, the MOBD samples were positioned directly beneath the penetration needle, which was allowed to penetrate the sample surface. The downward displacement of the needle during penetration was recorded as the penetration depth (d). The measured penetration depth (d) was subsequently used to determine the penetration resistance (P_r). Fig. 5 presents the spatial distribution of penetration resistance (P_r) for MOBD samples subjected to different EPs.

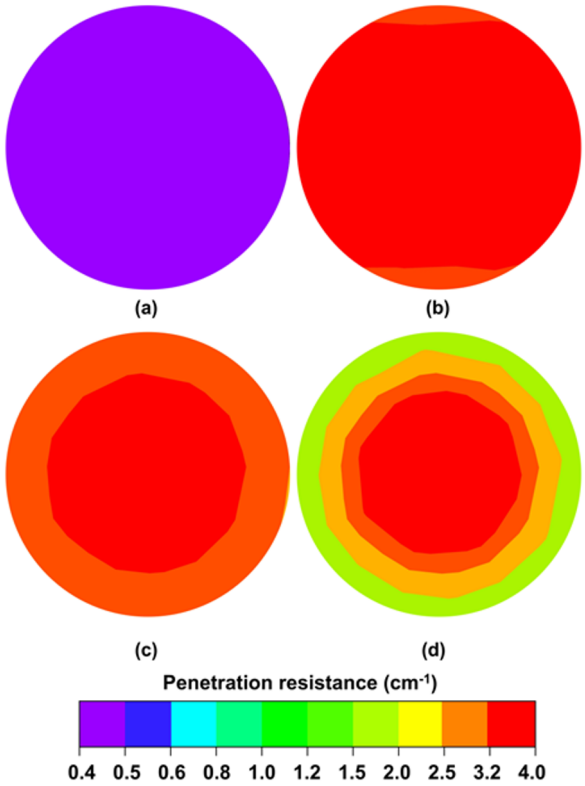

Fig. 5. Variation in the penetration resistance of (a) MOBD0; (b) MOBD1; (c) MOBD2; (d) MOBD3 sample.

The untreated MOBD0 sample, treated at 0 V with distilled water, exhibits a uniform penetration resistance of 4 cm^{-1} across the entire surface, indicating lowest penetration resistance (Fig. 5(a)). This response indicates limited surface stiffness and reflects the absence of electrochemical reactions or cementitious bonding in the untreated state. The uniformity of the stiffness distribution suggests a homogeneous but mechanically weak material structure, consistent with microstructural observations showing loosely packed particles without precipitation. In contrast, the MOBD1 sample treated with wetting fluid (WF) under an applied potential of 1 V shows a predominantly 4.0 cm^{-1} distribution. This significant increase in penetration resistance demonstrates the effectiveness of low-voltage electrical conditioning in enhancing surface stiffness. The improved resistance can be attributed to the initiation of ion migration and the formation of cementitious precipitates, such as calcium silicate hydrate (CSH), which promote interparticle bonding and restrict needle penetration. The relatively uniform stiffness further suggests that electrodeposition at 1 V

results in comparatively homogeneous stiffness development; similar observations have been made in microstructural analysis.

When the applied potential was increased to 3 V in the MOBD2 sample, a high penetration resistance value of 4 cm^{-1} remained, particularly in the central region between the electrodes. However, the outer regions exhibited a lower penetration resistance of 2 cm^{-1}, as indicated by the orange shades. Similarly, in the MOBD3 sample treated at 5 V exhibits the most pronounced spatial heterogeneity. This behaviour is consistent with the pH and microstructural observations, which show intensified electrolysis and a substantial reduction in pH at higher applied potentials. The acidic conditions generated in the inter-electrodic region, combined with accelerated ion transport, promote localized and premature precipitation of cementitious phases, resulting in dense but spatially confined bonding. In contrast, the peripheral regions experience limited ionic availability and disrupted CSH gel continuity, as evidenced by sparse and fragmented deposits in SEM images, leading to incomplete cementation despite the higher applied potential [19,20]. Overall, the penetration resistance results demonstrate that electrical conditioning significantly influences the mechanical response of MOBD. Higher applied voltages increase penetration resistance in the inter-electrode region; however, the outer zones consistently exhibit lower stiffness, underscoring the non-uniform nature of electrochemically induced cementation.

4 Conclusion

This study demonstrates that electrodeposition under mild electric potential (EP) is a promising and sustainable technique for improving the mechanical behaviour of mine overburden dump (MOBD) material. Microstructural analysis showed that low EP (1 V) promotes the formation of a uniform calcium silicate hydrate (CSH) gel, resulting in effective interparticle bonding, whereas higher EPs (3–5 V) lead to disrupted, non-uniform precipitates due to intensified electrolysis and ion transport. The pH measurements supported these findings, showing a progressive decrease in pH with increasing EP. The study establishes electrodeposition as a promising alternative for overburden stabilization, while emphasizing the need to carefully optimize electrical parameters and electrode configuration to ensure effective, durable field-scale implementation. Consequently, future optimization of electrode configuration, treatment duration, and electrical parameters is essential to achieve uniform and durable mechanical improvement in electrodeposition-treated MOBD.

5 References

1. S. Pandey, A.K. Jha, T.N. Singh, A sustainable approach for stabilization of coal mine overburden waste: a critical appraisal. Indian Geotech. J. **55**, 1301–1319 (2025). https://doi.org/10.1007/s40098-024-00987-6
2. O.A. Marín, A. Kraslawski, L.A. Cisternas, Estimating processing cost for the recovery of valuable elements from mine tailings using dimensional analysis. Miner. Eng. **184**, 107629 (2022). https://doi.org/10.1016/j.mineng.2022.107629
3. H.R. Manaviparast, J. Pinheiro, E.K. Najafi, C. Abreu, N. Araújo, N. Cristelo, T. Miranda, Mechanical behavior of a mine tailing stabilized with a sustainable binder. Appl. Sci. **13**, 4103 (2023). https://doi.org/10.3390/app13074103
4. T.K. Rajak, L. Yadu, S.K. Chouksey, P.K. Dewangan, Stability analysis of mine overburden dump stabilized with fly ash. Int. J. Geotech. Eng. **15**, 587–597 (2021). https://doi.org/10.1080/19386362.2018.1503780
5. Y. Izumi, A. Iizuka, H.-J. Ho, Calculation of greenhouse gas emissions for a carbon recycling system using mineral carbon capture and utilization technology in the cement industry. J. Clean. Prod. **312**, 127618 (2021). https://doi.org/10.1016/j.jclepro.2021.127618
6. V. Brar, D. Shirole, S. Das, Improvement and strengthening of silica sand with electric fields: an electrodeposition approach. Bull. Eng. Geol. Environ. **85**, 263 (2026). https://doi.org/10.1007/s10064-026-04885-4
7. V. Brar, S. Das, D. Shirole, Effects of mild direct current fields on the physical characteristics of silica sand, in Proceedings of the 13th Asian Rock Mechanics Symposium (ARMS13), New Delhi, India, September 22–27 (2024)
8. V. Brar, S. Das, D. Shirole, Electrodeposition and the action of electric gradient on soils: a comprehensive review. J. Appl. Electrochem. **55**, 1685–1703 (2025). https://doi.org/10.1007/s10800-025-02274-5
9. A. Landivar Macias, S.D. Jacobsen, A.F. Rotta Loria, Electrodeposition of calcareous cement from seawater in marine silica sands. Commun. Earth Environ. **5**, 442 (2024). https://doi.org/10.1038/s43247-024-01604-3
10. R.A. García-Gaines, S. Frankenstein, USCS and the USDA soil classification system: development of a mapping scheme (Defense Technical Information Center, Fort Belvoir, VA, 2015). https://doi.org/10.21236/ADA614144
11. D. Hou, H. Ma, Z. Li, Morphology of calcium silicate hydrate (C-S-H) gel: a molecular dynamic study. Adv. Cem. Res. **27**, 135–146 (2015). https://doi.org/10.1680/adcr.13.00079
12. W.A. Hunnicutt, Characterization of calcium-silicate-hydrate and calcium-alumino-silicate-hydrate, M.S. thesis, University of Illinois at Urbana-Champaign, 2013
13. P. Bera, H. Seenivasan, K.S. Rajam, V.K. William Grips, XRD, FESEM and XPS studies on heat treated Co-W electrodeposits. Mater. Lett. **76**, 103–105 (2012). https://doi.org/10.1016/j.matlet.2012.02.046
14. C.-Y. Ou, S.-C. Chien, C.-C. Yang, C.-T. Chen, Mechanism of soil cementation by electroosmotic chemical treatment. Appl. Clay Sci. **104**, 135–142 (2015). https://doi.org/10.1016/j.clay.2014.11.020
15. A.L. Ayodele, S. Pamukcu, R.A. Shrestha, O.A. Agbede, Electrochemical soil stabilization and verification. Geotech. Geol. Eng. **36**, 1283–1293 (2018). https://doi.org/10.1007/s10706-017-0392-8
16. Y. Tang, N. Wang, T. Liu, Electrokinetic stabilization of marine clayey soils by different injection procedures. Int. J. Electrochem. Sci. **16**, 210223 (2021). https://doi.org/10.20964/2021.02.24
17. A.N. Alshawabkeh, T.C. Sheahan, Soft soil stabilisation by ionic injection under electric fields. Proc. Inst. Civ.

Eng. Ground Improv. **7**, 177–185 (2003). https://doi.org/10.1680/grim.2003.7.4.177
18. X. Shen, P. Feng, Q. Zhang, J. Lu, X. Liu, Y. Ma, P. Jin, W. Wang, Q. Ran, J. Hong, Toward the formation mechanism of synthetic calcium silicate hydrate (C-S-H) – pH and kinetic considerations. Cem. Concr. Res. **172**, 107248 (2023). https://doi.org/10.1016/j.cemconres.2023.107248
19. F. Sadeghian, S. Jahandari, A. Haddad, H. Rasekh, J. Li, Effects of variations of voltage and pH value on the shear strength of soil and durability of different electrodes and piles during electrokinetic phenomenon. J. Rock Mech. Geotech. Eng. **14**, 625–636 (2022). https://doi.org/10.1016/j.jrmge.2021.07.017
20. P. Asavadorndeja, U. Glawe, Electrokinetic strengthening of soft clay using the anode depolarization method. Bull. Eng. Geol. Environ. **64**, 237–245 (2005). https://doi.org/10.1007/s10064-005-0276-7